Journal of Alloys and Compounds 509 (2011) 1947–1952

Contents lists available at ScienceDirect

Journal of Alloys and Compounds

journal homepage: www.elsevier.com/locate/jallcom

Optical, structural and surface characterization of ultrasonically sprayed CdO:F films

I. Akyuz [a], S. Kose [a], E. Ketenci [b], V. Bilgin [c], F. Atay [a,*]

[a] Eskisehir Osmangazi University, Department of Physics, 26480 Eskisehir, Turkey
[b] Eskisehir Osmangazi University, Graduate School of Science, 26480 Eskisehir, Turkey
[c] Canakkale Onsekiz Mart University, Department of Physics, 17100 Canakkale, Turkey

ARTICLE INFO

Article history:
Received 25 February 2010
Received in revised form
20 September 2010
Accepted 19 October 2010
Available online 30 October 2010

Keywords:
Ultrasonic spray pyrolysis
CdO:F
Thin film
Spectroscopic ellipsometry
XRD
AFM

ABSTRACT

In this work, we report the effect of F doping on some physical properties of CdO films. Ultrasonic spray pyrolysis technique has been used to obtain the films. Thicknesses, refractive indices and extinction coefficients of the films have been determined by spectroscopic ellipsometry technique using Cauchy–Urbach model for fitting. Transmission and reflectance spectra have been taken by UV spectrophotometer, and band gap values have been determined by optical method. X-ray diffraction patterns have been used to study the structural properties such as crystallinity level, texture coefficient, crystallite size and lattice constants. Atomic force microscope images have been taken to see the effect of F doping on surface topography and roughness of CdO films. Finally, it has been concluded that both of the F doped CdO films have improved properties and are promising materials for solar cell applications.

1. Introduction

Materials exhibiting high electrical conductivity, optical transparency and that can be grown efficiently as thin films are used extensively for variety of applications [1] such as photovoltaic solar cells [2], phototransistors [3], photodiodes [4], gas sensors [5], etc. CdO thin films have great technological interest due to their high-quality and optical properties [6]. CdO is an n-type semiconducting material with band gap energy between 2.2 and 2.7 eV [7,8]. The impurities used as doping agents for CdO films are fluorine [9–12], aluminum [13], tin [14,15] and indium [14]. Many methods have been employed to prepare CdO thin films like sputtering [16,17], thermal evaporation [18], laser ablation [19], spray pyrolysis [20–22], sol–gel [23], MOCVD [24]. Among these techniques, spray pyrolysis competes with the others due to its low cost and suitable properties and this technique is a process well suited to large-scale production [20,24,25].

Transparent conducting oxide (TCO) technology needs new and alternative materials with improved characteristics. Use of a low-cost technique is also important for cost-reduction purposes. CdO is a promising material with its high mobility as compared to other TCOs. But, it is not preferred due to its moderate bang gap of ~2.2 eV. With respect to this aim, we have tried to improve the characteristics (especially increasing the band gap) by F incorporation. Also, we have used an ultrasonic spray pyrolysis (USP) set-up which is simple and economic, allow doping of different elements and deposition onto large-areas without the need for vacuum.

2. Experimental details

2.1. Film formation

Ultrasonic spray pyrolysis (USP) technique was used to deposit undoped and F doped CdO films. Details of the USP technique were given in our previous works [26,27]. The ultrasonic oscillator frequency was 100 kHz, and the droplet size was 20 μm. Heated microscope glasses (Objekttrager, 1 cm × 1 cm) were used as substrate. Substrate heating was performed by an electrical heater, and the substrate temperature was controlled with an iron-constantan thermocouple. $Cd(CH_3COO)_2{\cdot}2H_2O$ and NH_4F (ammonium fluoride) solutions were used as Cd and F sources, respectively. Deionized water was used as the solvent. The starting spraying solution was mixed and heated (30 °C) with a magnetic mixer to prevent sedimentation. Details of other experimental parameters are given in Table 1. The samples have been named as CF0 (undoped CdO), CF2 (F doped at 2%) and CF4 (F doped at 4%). F doping percentages represent the amount in the starting solutions.

2.2. Film characterization

In spectroscopic ellipsometry (SE) measurements, two parameters, ψ and Δ, are measured as a function of the wavelength (or photon energy) from a given sample. These two parameters are related to the optical and structural properties of the

* Corresponding author. Tel.: +90 222 239 37 50x2825; fax: +90 222 239 35 78.
E-mail addresses: iakyuz@ogu.edu.tr (I. Akyuz), skose@ogu.edu.tr (S. Kose), eketenci@ogu.edu.tr (E. Ketenci), vbilgin@comu.edu.tr (V. Bilgin), fatay@ogu.edu.tr (F. Atay).

0925-8388/$ – see front matter © 2010 Elsevier B.V. All rights reserved.
doi:10.1016/j.jallcom.2010.10.097

Table 1
Details of experimental parameters used to produce CdO:F films.

Material	CdO:F
Sample codes	CF0, CF2, CF4
Doping level (at%)	0, 2 and 4
Source solutions	$Cd(CH_3COO)_2{\cdot}2H_2O$ and FH_4N
Molarity	0.1 M
Total volume of spraying solution	150 cm^3
Substrate temperature	$300 \pm 5\,^{\circ}C$
Solution flow rate	5 $cm^3\ min^{-1}$
Spraying time	30 min
Nozzle to substrate distance	25 cm
Carrier gas/pressure	Air/1 bar

sample through the following expression;

$$\rho = \frac{R_p}{R_s} = \tan\,\psi\,\exp(i\Delta) \quad (1)$$

where R_p and R_s are the complex reflection coefficients for the light polarized parallel (p) and perpendicular (s) to the plane of incidence, respectively [28].

PHE-102 spectroscopic ellipsometer (250–2300 nm) was used to determine the Ψ parameters, refractive indices (n) and thicknesses (d) of the films. Cauchy–Urbach dispersion model was used to fit the experimental Ψ parameters. This model is a modified type of Cauchy model. In the Cauchy–Urbach dispersion model, the refractive index $n(\lambda)$ and the extinction coefficient $\kappa(\lambda)$ as a function of the wavelength are given by,

$$n(\lambda) = A + \frac{B}{\lambda^2} + \frac{C}{\lambda^4} \quad (2)$$

$$\kappa(\lambda) = \alpha\,\exp\,\beta\left(12,400\left(\frac{1}{\lambda} - \frac{1}{\gamma}\right)\right) \quad (3)$$

where A, B, C, α, β and γ are model parameters [29]. Cauchy–Urbach model may be used for samples with low absorption. So, we performed our measurements between 1200 and 1600 nm wavelength range where the films have low absorption. For the samples having depolarization effect, the incident angle is an important factor. This will affect the intensity and phase of the reflected light which then goes to the analyzer. Six different incident angles (50°, 55°, 60°, 65°, 70°, 75°) were tried to take the measurements. The best angle was determined to be 75° using experimental Ψ spectra. Then, the parameters (A, B, C, α, β) related to the Cauchy–Urbach model were determined.

Shimadzu-SolidSpec-3700 UV-VIS-NIR spectrophotometer was used to take transmittance (T) and reflectance (R) spectra. Also, band gap values of the films were determined by optical method.

Rigaku X-ray diffractometer with CuKα radiation between $20^{\circ} \le 2\theta \le 80^{\circ}$ was used for X-ray diffraction studies. Crystallinity levels of the films were investigated, and some structural parameters such as lattice constants, texture coefficient and crystallite size were determined.

Park System XE-70 AFM was used to take surface images. The measurements were taken in non-contact mode, ~300 kHz frequency and 0.55 Hz scan rate in air at room temperature. A silicon cantilever which has a spring constant of 40 N/m was used. Also, root mean square (rms, R_q), average (R_a) and peak to valley (R_{pv}) roughness values were obtained using XEI version 1.7.1 software. All the images were taken from an area of 2.5μm × 2.5 μm. The roughness values belong to whole scanned area.

3. Results and discussion

SE spectra of CdO:F films on glass substrates in the wavelength range of 1200–1600 nm are shown in Fig. 1. The experimental data were analyzed using the Cauchy–Urbach model, and a good fit is found between the model and experimental data. However, it was determined that there are some deviations on fitted Ψ values probably caused by the roughness, grain boundaries and morphology of the samples. Also, the rough surface and backsides of the samples may affect the reflection of light. Besides, the grain boundaries and morphologies would depolarize the incident polarized light, resulting deviated experimental ellipsometric parameters and deteriorating the SE fitting [30]. Thicknesses, refractive indices and extinction coefficients of all films have been determined using these Ψ spectra. These values and model parameters are given in Table 2. It was determined that F doping caused the thickness values to increase. Besides, there is a little increase in the average refractive index value of CF4 films as compared to CF0. The little change in the refractive index of the samples is due to the change in reflectance values. When we look at the reflectance spectra between 1200 and 1600 nm wavelength ranges, it is clear that CF4 has higher reflectance than other films and CF2 has the lowest reflectance value. This supports the refractive index values of same samples, as CF4 having the highest refractive index value. Probably, the good packing density of CF4 on the surface caused this sample to have the highest reflectance and refractive index values. It was also determined from Table 2 that F doping caused the extinction

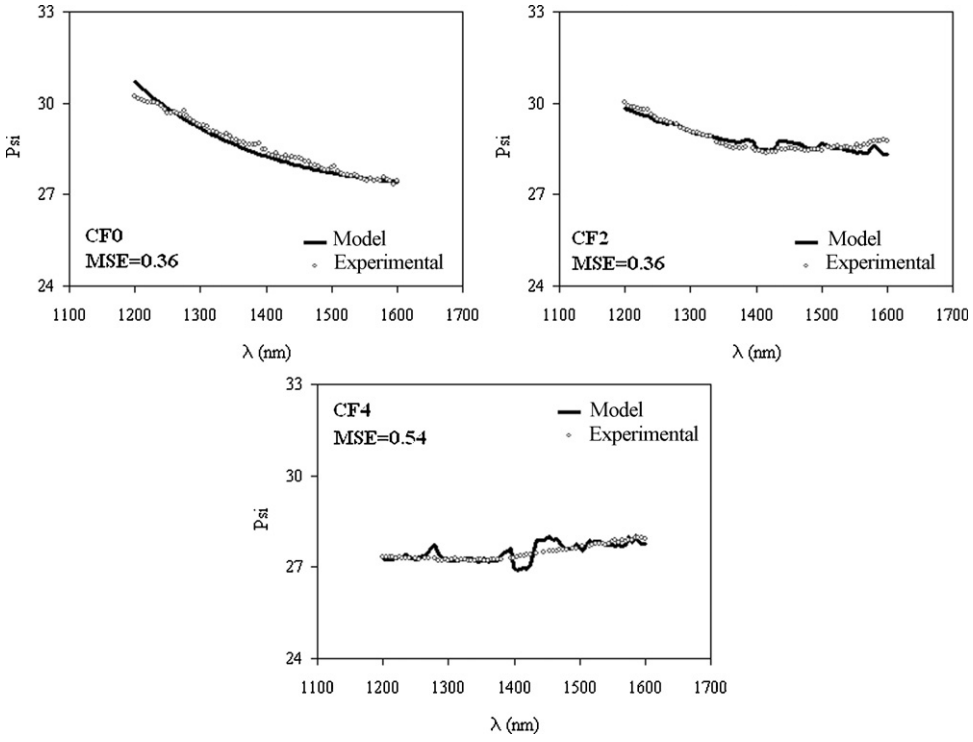

Fig. 1. SE spectra of CdO:F films.

Table 2
Thicknesses, model parameters, mean square error (MSE) values, average refractive indices and average extinction coefficients of CdO:F films.

Material	d (nm)	A	B ($\times10^{-2}$) (nm)^2	C ($\times10^{-2}$) (nm)^4	α	β (nm)	MSE	n	k
CF0	538	1.687	−55.2	9.1	0.043	3.59	0.36	1.42	1.30
CF2	684	1.597	−39.8	3.2	0.002	1.55	0.36	1.39	0.16
CF4	623	1.380	18.3	−3.6	0.031	2.18	0.54	1.47	0.02

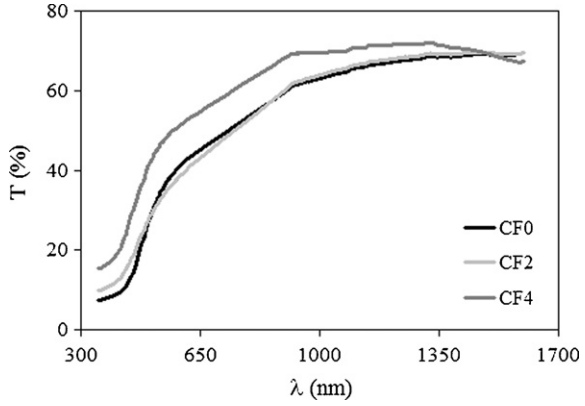

Fig. 2. The transmittance spectra of CdO:F films.

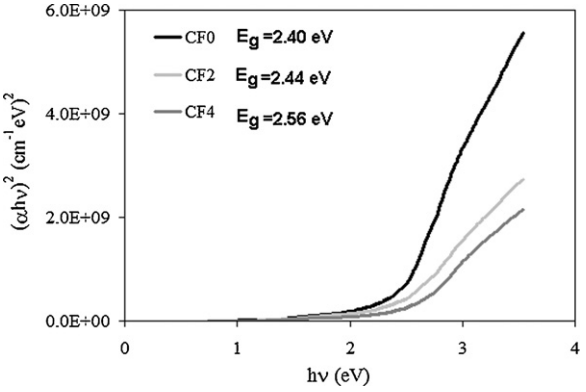

Fig. 4. $(\alpha h\nu)^2 \sim h\nu$ plots of CdO:F films.

coefficient to decrease, and the extinction coefficient of a material is directly related to its absorption characteristic.

The transmittance and reflectance spectra of CF films are given in Figs. 2 and 3, respectively. F doping at 4% showed higher transmittance as compared to others. There is not a linear variation in reflectance values with F doping. The lowest reflectance value has been obtained for sample CF2.

Band gap values of all films have been determined by optical method using $(\alpha h\nu)^2 \sim h\nu$ plots given in Fig. 4. F doping caused the band gap values to increase. This is an improvement for solar cell applications as the studies on CdO concentrate on increasing the low band gap value as compared to other TCOs.

Fig. 5 shows the XRD patterns of the sample. The data related to the peaks with different intensities and widths on these patterns is given in Table 3. All the films have polycrystalline structures. There are three intensive peaks which belong to the reflections from (1 1 1) CdO_2, (1 1 1) CdO and (2 0 0) CdO planes. This shows the films contain two phases as CdO_2 and CdO. We think that these phases have been formed as a result of the chemical reaction during the deposition process. It is previously mentioned in the literature that there are three possible charge states for the interstitial oxygen as (i) null effective charge (ii) single negatively charged (iii) doubly negatively charged [31]. As a result of the chemical reaction during the experiment, oxygen would probably join the lattice as interstitial having single negative charge and caused the formation of CdO_2 phase. We know that from our previous experiences that this phase is an unstable phase and can disappear after thermal treatments. Peaks with high intensities and narrow full width half maximums show that the crystallinity levels of the films are good.

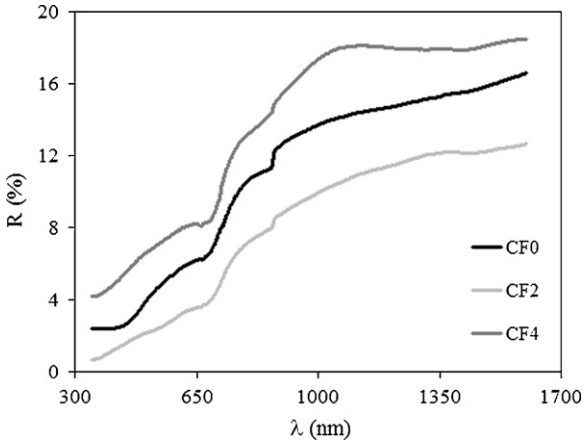

Fig. 3. The reflectance spectra of CdO:F films.

XRD patterns show that the degree of orientation of different planes is not similar. In order to investigate a possibility of the preferred orientation, the Harris analysis was performed [32,33]. The calculated texture coefficient (TC) values are given in Table 3. It was determined that all films have three TC values bigger than one. This means they have dominant growth directions through three different planes. Crystallite size (D) values have been determined for both of the phases (CdO and CdO_2) using Scherrer's formula [34] and listed in Table 3. There is a little decrease in the crystallite size of CdO_2 phase with F doping.

Lattice parameters for all samples have been determined for the orientations with highest TC value and compared with the ones in ASTM (American Society of Testing Materials) cards. These values are given in Table 4. A good agreement is found between these two values.

AFM images of all films are shown in Fig. 6. A granular structure with grains in different sizes is dominant for CF0 films. White regions in this figure represent the formation of agglomerated grains one on the top of the other. For these white regions, we think that neighboring grains come together forming large clusters. So, grains in the white regions are larger in size as compared to others. From all of these interpretations, film growth mechanism is thought to be formed firstly layer by layer and then island growth type (mixed growth). It was determined from AFM images of CF0 films that there are also black regions which represent the grain cavities on the film surface. Probably, atoms coming to the surface do not prefer these regions as growth centers and migrate to the white regions with bigger atom groups by surface diffusion. Also, the glass substrate has roughness on its surface. Regions on the substrate surface such as hollows, valleys and step outsets behave like a high energy barrier for the atoms which tend to leave from the surface. So, these are appropriate regions where defects and atoms of the film tend to nucleate. Thus, the substrate also affects

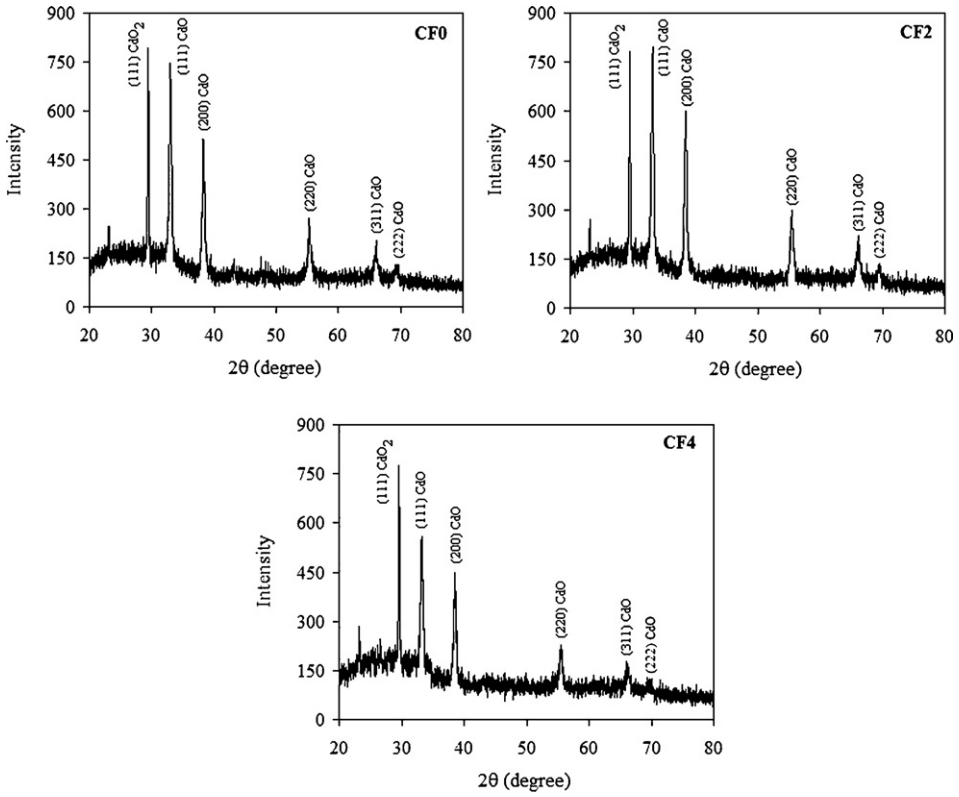

Fig. 5. XRD patterns of CdO:F films.

Table 3
The data related to the peaks with different intensities and widths on XRD patterns.

Material	2θ (°)	d (Å)	I/I_0	($h\,k\,l$)	Crystal system	TC	$B \times 10^{-3}$ (radian)	D (Å)
	29.42	3.034	100.00	(1 1 1)	CdO_2 cubic	1.93	3.16	474
	32.99	2.712	96.70	(1 1 1)	CdO cubic	1.87	6.94	217
CF0	38.34	2.346	67.20	(2 0 0)	CdO cubic	1.30	7.12	215
	55.32	1.659	24.90	(2 2 0)	CdO cubic	0.48	7.92	206
	66.00	1.414	15.10	(3 1 1)	CdO cubic	0.29	10.40	165
	29.52	3.023	100.00	(1 1 1)	CdO_2 cubic	1.84	3.35	447
	33.16	2.699	99.70	(1 1 1)	CdO cubic	1.83	7.01	215
CF2	38.50	2.336	71.70	(2 0 0)	CdO cubic	1.32	7.38	207
	55.52	1.654	30.00	(2 2 0)	CdO cubic	0.55	8.41	194
	66.10	1.412	19.40	(3 1 1)	CdO cubic	0.36	8.62	200
	29.60	3.016	100.00	(1 1 1)	CdO_2 cubic	2.40	3.16	474
	33.16	2.699	63.70	(1 1 1)	CdO cubic	1.53	7.10	212
CF4	38.50	2.336	50.70	(2 0 0)	CdO cubic	1.22	8.08	189
	55.58	1.652	19.00	(2 2 0)	CdO cubic	0.46	8.90	183
	65.99	1.414	10.10	(3 1 1)	CdO cubic	0.24	9.86	175

the homogeneity of the surface and size of the grains. F doping showed itself as an increase in the agglomerated regions, which in turn increases the grain cavities. For CF2 film, agglomerated areas have waterway-like and sharp formations. F doping at 4% caused the formation of grains which are smaller in size and difficult to detect. This film also has mount-like grains on its surface. R_q, R_a and R_{pv} values of CdO:F films are given in Table 5. It is clear that F doping affected the roughness values of CF films.

The current values of CdO:F films were measured at room temperature in the dark by applying voltage values between 0.1 and 10 V. Electrical resistivity and conductivity values of the films were calculated using two-probe method and are given in Table 6. A noticeable increase in resistivity value of CF4 film could probably due to the dominant amount of CdO_2 phase in this film. We think that increased number of oxygen interstitials which behave as scattering centers affected the mobility of the carriers and increased

Table 4
Lattice parameters, d and B values for CdO:F films.

Material	Dominant orientation	d (Å)	$B \times 10^{-3}$ (radian)	Calculated $a = b = c$ (Å)	ASTM $a = b = c$ (Å)
CF0	(1 1 1) CdO_2	3.034	3.16	5.254	5.313
CF2	(1 1 1) CdO_2	3.023	3.35	5.237	5.313
CF4	(1 1 1) CdO_2	3.016	3.16	5.223	5.313

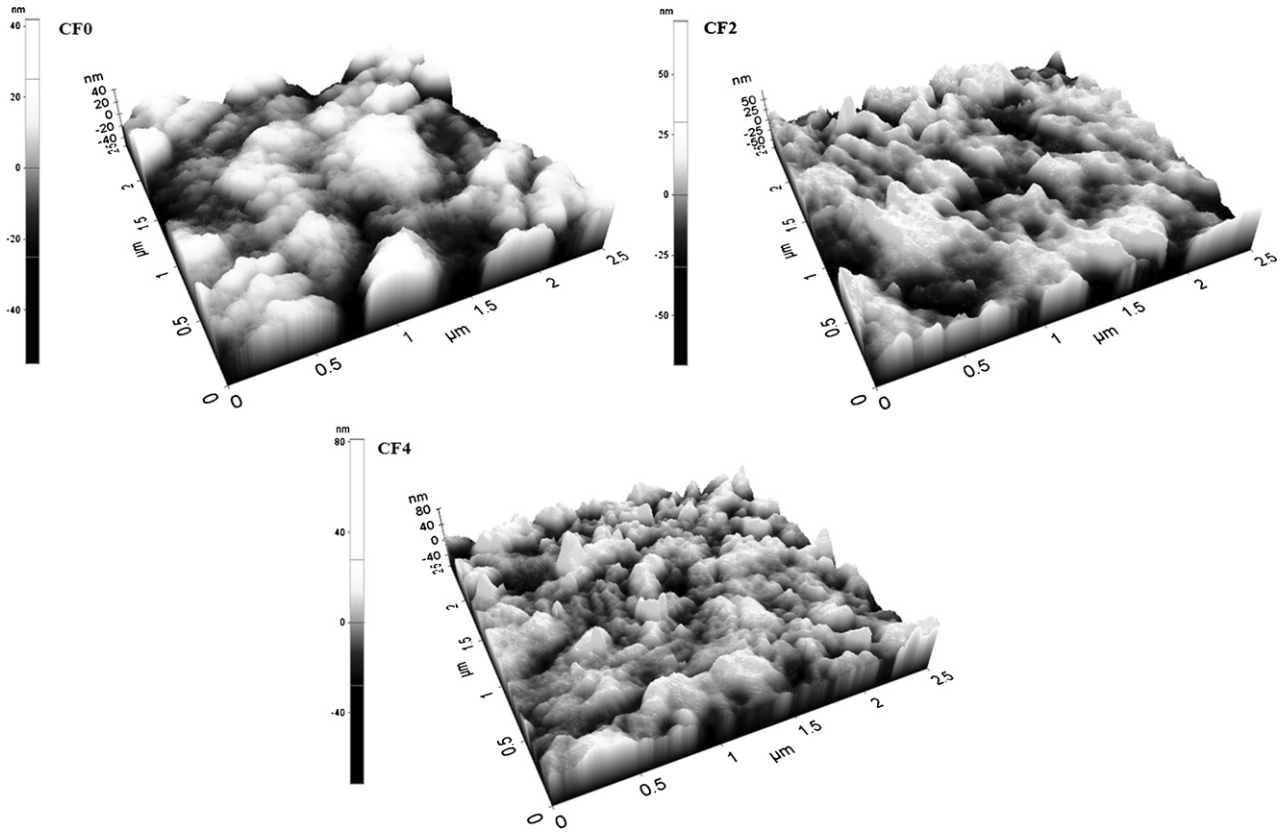

Fig. 6. AFM images of CdO:F films.

Table 5
R_q, R_a and R_{pv} roughness values of CdO:F films.

Material	R_q (nm)	R_a (nm)	R_{pv} (nm)
CF0	12	10	96
CF2	15	12	142
CF4	18	13	172

Table 6
Electrical resistivity and conductivity values of CdO:F films.

Material	$\rho\,(\Omega\,\mathrm{cm})^{-1}$	$\sigma\,(\Omega\,\mathrm{cm})^{-1}$
CF0	8.41×10^{-4}	1.19×10^{3}
CF2	8.90×10^{-4}	1.12×10^{3}
CF4	4.44×10^{-2}	2.25×10^{1}

the resistivity value of this film. Another reason for the increase in resistivity may be the electron–electron or electron–impurity scattering which probably induced by F doping. Especially for CF4 film which has the highest reflectance value, increasing number of carriers may cause an increase in resistivity because of these scattering mechanisms. So, increasing band gap with F doping might be the effect of Moss–Burstein effect.

4. Conclusion

In this work, the effect of F doping on the optical, structural and surface properties of ultrasonically sprayed CdO films has been investigated. F doping affected each of these properties. Firstly, the low cost of the production system is an advantage for potential applications of these films. CF4 film caused the transmittance values to increase which is a desired development for transparent conducting oxide industry. Low reflectance value of CF2 film makes this sample a promising material for anti-reflection coatings. Also at the end of our investigations, F doping has found to be an alternative solution to increase the narrow band gap of CdO films. This is an other development of CdO:F films for optoelectronic and photovoltaic solar cell applications. The surface of undoped film modified to have a grained texture with smaller grains by F doping. There is a disadvantage of F doped samples as having a little higher roughness value as compared to the undoped one. But, post-deposition processing such as annealing in different atmospheres may probably decrease the roughness and these doped films become promising materials for solar cell applications. However, rough samples may be an alternative in single-junction μc-Si solar cells having superstrate configuration. When we take into account the refractive index and rough surface of the samples, rough interface between a low refractive index material (CdO:F, $n \sim 1.6$) and a high refractive index material (for Si $n \sim 3.7$) results in reduced reflection due to gradual refractive index matching. In order to increase this effect high rms roughness (R_q) values needed. Also this will allow light trapping into Si layer and cause back and forth scattering at the interfaces increasing the optical path within the Si layer. The most important characteristics for TCO films in photovoltaic applications are high transparency and low resistivity. With respect to this aim, we try to determine a quality factor (Φ) for the films including average transmittance (at 350–1600 nm) and sheet resistance (R_s) values using Haacke's figure of merit ($\Phi = T^{10}/R_s$) [35]. The Φ values of all films were calculated as 1.62×10^{-4}, 2.33×10^{-4} and $1 \times 10^{-5}\,(\Omega)^{-1}$, respectively. The values of the figure of merit are comparable with results reported by Kul et al. [22].

Acknowledgement

This work was supported by TUBITAK (The Scientific and Technological Research Council of Turkey) under the project number 108T525.

References

[1] R.R. Salunkhe, D.S. Dhawale, T.P. Gujar, C.D. Lokhande, Materials Research Bulletin 44 (2009) 364.
[2] R.S. Mane, H.M. Pathan, C.D. Lokhande, S.H. Han, Solar Energy 80 (2006) 185.
[3] L.M. Su, N. Grote, F. Schmitt, Electronics Letters 20 (1984) 716.
[4] R. Kondo, H. Okhimura, Y. Kasai, Japanese Journal of Applied Physics 10 (1971) 1547.
[5] V.R. Shinde, T.P. Gujar, C.D. Lokhande, R.S. Mane, S.H. Han, Materials Science and Engineering B 1 (2007) 119.
[6] M.A. Flores, R. Castanedo, G. Torres, O. Zelaya, Solar Energy Materials and Solar Cells 93 (2009) 28.
[7] K.L. Chopra, S. Ranjan Das, Thin Film Solar Cells, Plenum Press, NY, 1993.
[8] Y.S. Choi, C.G. Lee, S.M. Cho, Thin Solid Films 289 (1996) 0153.
[9] J. Santos Cruz, G. Torres Delgado, R. Castanedo Perez, S. Jimenez Sandoval, J. Marquez Marin, O. Zelaya Angel, Solar Energy Materials and Solar Cells 90 (2006) 2272.
[10] J. Santos Cruz, G. Torres Delgado, R. Castanedo Perez, C.I. Zuniga Romero, O. Zelaya Angel, Thin Solid Films 515 (2007) 5381.
[11] P.K. Ghosh, R. Maity, K.K. Chattopadhyay, Solar Energy Materials and Solar Cells 81 (2004) 279.
[12] R. Ferro, J.A. Rodriguez, Thin Solid Films 347 (1999) 295.
[13] R. Maity, K.K. Chattopadhyay, Solar Energy Materials and Solar Cells 90 (2006) 597.
[14] C.S. Ferekides, R. Mamazza, U. Balasubramanian, D.L. Morel, Thin Solid Films 480 (2005) 224.
[15] X. Wu, T.J. Cotts, W.P. Mulligan, Journal of Vacuum Science and Technology A 15 (1997) 1057.
[16] T.K. Subramanyam, S. Uthanna, B. Sinivasulu Naidu, Materials Letters 35 (1998) 214.
[17] K. Gurumurugan, D. Mangalaraj, Sa.K. Narayandass, Journal of Electronic Materials 25 (1996) 765.
[18] M. Dinesau, P. Verardi, Applied Surface Science 106 (1996) 149.
[19] C. Messaoudi, D. Sayah, Abd-Lafdil, Physica Status Solidi A 151 (1995) 93.
[20] B. Ergin, E. Ketenci, F. Atay, International Journal of Hydrogen Energy 34 (2009) 5249.
[21] R. Kumaravel, V. Krishnakumar, K. Ramamurthi, E. Elangovan, M. Thirumavalavan, Thin Solid Films 515 (2007) 4061.
[22] M. Kul, A.S. Aybek, E. Turan, M. Zor, S. Irmak, Solar Energy Materials and Solar Cells 91 (2007) 1927.
[23] A.A. Dakhel, A.Y. Ali-Mohamed, Materials Chemistry and Physics 113 (2009) 356.
[24] V. Bilgin, S. Kose, F. Atay, I. Akyuz, Materials Letters 58 (2004) 3686.
[25] O.B. Ajayi, O.K. Osuntola, I.A. Ojo, C. Jeynes, Thin Solid Films 248 (1994) 57.
[26] F. Atay, S. Kose, V. Bilgin, I. Akyuz, Materials Letters 57 (2003) 3461.
[27] F. Atay, V. Bilgin, I. Akyuz, S. Kose, Materials Science in Semiconductor Processing 6 (2003) 197.
[28] F.K. Shan, Z.F. Liu, G.X. Liu, B.C. Shin, Y.S. Yu, S.Y. Kim, T.S. Kim, Journal of Korean Physical Society 44 (2004) 1215.
[29] M.J. Khoshman, E.M. Kordesch, Journal of Non-Crystalline Solids 351 (2005) 3334.
[30] N. Ueda, H. Maeda, H. Hosono, H. Kawazoe, Journal of Applied Physics 84 (1998) 6174.
[31] A.C.S. Sabioni, Solid State Ionics 170 (2004) 145.
[32] C.S. Barrett, T.B. Massalski, Structure of Metals, Pergamon, Oxford, 1980, p. 204.
[33] V. Bilgin, S. Kose, F. Atay, I. Akyuz, Journal of Materials Science 40 (2005) 1909.
[34] A.S. Riad, S.A. Mahmoud, A.A. Ibrahim, Physica B 296 (2001) 319.
[35] G. Haacke, Journal of Applied Physics 47 (1976) 4086.